ANTICANCER RESEARCH *39*: 3507-3518 (2019)
doi:10.21873/anticanres.13497

Quantitative Structure–Cytotoxicity Relationship of Azulene Amide Derivatives

KANA IMANARI[1], MASASHI HASHIMOTO[1], HIDETSUGU WAKABAYASHI[1], NORIYUKI OKUDAIRA[2], KENJIRO BANDOW[3], JUNKO NAGAI[4], MINEKO TOMOMURA[3], AKITO TOMOMURA[3], YOSHIHIRO UESAWA[4] and HIROSHI SAKAGAMI[5]

[1]Faculty of Science, Josai University, Sakado, Japan;
Division of [2]Pharmacology and [3]Biochemistry, and [5]Meikai University Research Institute of Odontology (M-RIO), Meikai University School of Dentistry, Sakado, Japan;
[4]Department of Medical Molecular Informatics, Meiji Pharmaceutical University, Tokyo, Japan

Abstract. *Background/Aim: Very few studies of anticancer activity of azulene amides led us to investigate the cytotoxicity of 21 N-alkylazulene-1-carboxamides introduced either with 3-methyl **[1-7]**, 7-isopropyl-3-methyl **[8-14]** or 2-methoxy group **[15-21]**. Materials and Methods: Tumor-specificity (TS) was calculated by the ratio of mean 50% cytotoxic concentration (CC_{50}) against three normal human oral mesenchymal cells to that against four human oral squamous cell carcinoma (OSCC) cell lines. Potency-selectivity expression (PSE) was calculated by dividing TS value by CC_{50} value against OSCC cell lines. Apoptosis-inducing activity was evaluated by caspase-3 activation and appearance of subG$_1$ cell population. Results: **[8-14]** showed higher TS and PSE values, than **[1-7]** and **[15-21]**. The most active compound **[8-14]** induced apoptosis in C9-22 OSCC cells at 4-times higher CC_{50}. Quantitative structure-activity relationship analysis of **[1-14]** demonstrated that their tumor-specificity was correlated with chemical descriptors that explain the molecular shape and hydrophobicity. Conclusion: 7-Isopropyl-3-methyl-N-propylazulene-1-carboxamide **[8]** can be a potential candidate of lead compound for manufacturing new anticancer drug.*

Azulene, an isomer of naphthalene, is well known for its beneficial antioxidant effects. Azulene gargle has been used to reduce the incidence of undesirable general anesthesia-induced postoperative sore (1). Sodium azulene sulfonate, a water-soluble derivative of azulene, inhibited the capsaicin-induced pharyngitis in rats, possibly by its antioxidative effect (2). Administration of 6-isopropyl-3-[4-(4-chlorophenylsulfonylamino)butyl]azulene-1-sulfonic acid sodium salt (KT2-962), a thromboxane A receptor antagonist, significantly reduced the myocardial ischemia/reperfusion injury in a dog, possibly by its direct hydroxyl radical scavenging activity (3). Azulenic retinobenzoic acid derivatives effectively suppressed the carcinogen-induced neoplastic transformation of mouse fibroblast C3H/10T1/2 cells (4). Guaiazulene, a lipophilic azulene derivative which is abundant in nature, protected rats from paracetamol-induced hepatocytotoxicity by its antioxidant activity (inhibition of lipid peroxidation and radical scavenging action) (5). Guaiazulene also inhibited CYP1A2 that participates in the formation of toxic metabolite *N*-acetyl-p-benzoquinone imine (NAPQI) and the metabolic activation of several toxic and carcinogenic compounds (6). On the other hand, there is a limited number of studies that have investigated the cytotoxicity of guaiazulene against human malignant (7-9) and non-malignant cells (9, 10).

We recently reported that among ten azulene-related compounds, *N*-propylguaiazulenecarboxamide showed the highest tumor-specificity against human oral squamous cell carcinoma (OSCC) cell lines (Ca9-22, HSC-2, HSC-3, HSC-4) *vs.* three normal human oral mesenchymal cells (gingival fibroblast, HGF; periodontal ligament fibroblast, HPLF; pulp cell, HPC) (10). Furthermore, quantitative structure-activity relationship (QSAR) analysis demonstrated the tight correlation between their tumor-specificity and hydrophobicity and molecular shape (11). PubMed search revealed only one study that has investigated the anticancer activity of azulene amides (10).

In order to obtain more tumor-selective guaiazulene derivatives, we have synthesized a total of 21 *N*-alkylazulene-

Correspondence to: Hidetsugu Wakabayashi, Faculty of Science, Josai University, 1-1 Keyakidai, Sakado, Saitama 350-0295, Japan. Tel: +81 492717959, Fax: +81 492717985, e-mail: hwaka@josai.ac.jp/ sakagami@dent.meikai.ac.jp

Key Words: QSAR, Azulene amides, oral squamous cell carcinoma, apoptosis tumor specificity, chemical descriptor, hydrophobicity, molecular shape.

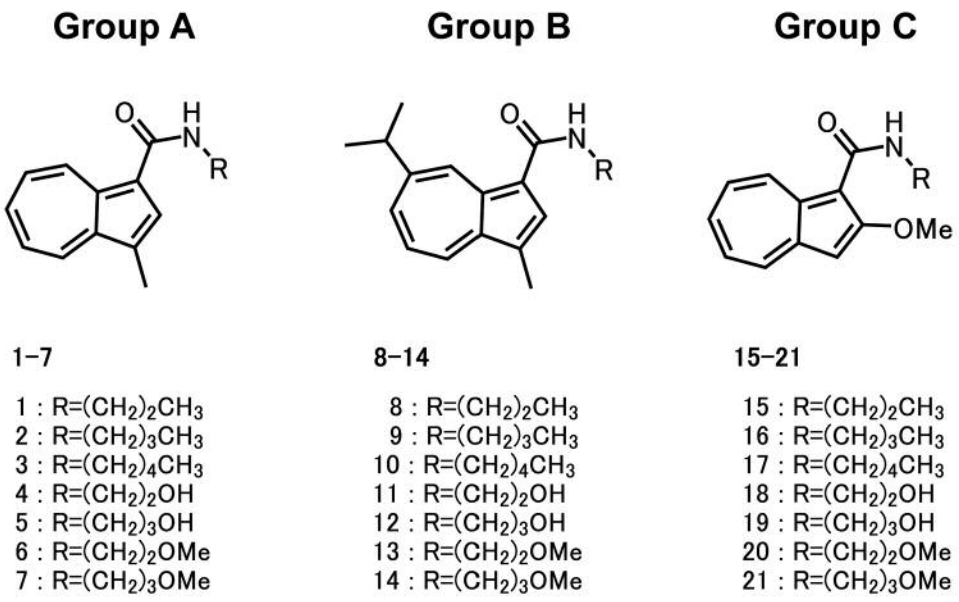

Figure 1. *Structure of three groups of azulene amide derivatives used in this study.*

1-carboxamide where 3-methyl, 7-isopropyl-3-methyl or 2-methoxy groups were introduced (Figure 1) and investigated their anticancer activity using four human oral squamous cell carcinoma (OSCC) cell lines and three normal human oral mesenchymal cells. We also investigated the effect of these compounds on apoptosis induction, since many anticancer drugs have been reported to induce apoptosis in clinical cancer tissues (12).

Materials and Methods

Materials. The following chemicals were obtained from the indicated companies: Dulbecco's modified Eagle's medium (DMEM) from GIBCO BRL (Grand Island, NY, USA); fetal bovine serum (FBS), 3-(4,5-dimethylthiazol-2-yl)-2,5-diphenyltetrazolium bromide (MTT), doxorubicin-HCl (DXR) from Sigma-Aldrich Inc., (St. Louis, MO, USA); dimethyl sulfoxide (DMSO), actinomycin D (Act. D) from Wako Pure Chem. Ind., (Osaka, Japan); culture plastic dishes and 96-well plates from Techno Plastic Products AG, (Trasadingen, Switzerland). Protease and phosphatase inhibitors were purchased from Roche Diagnostics (Tokyo, Japan).

Synthesis of alkylaminogroups. 3-methyl-*N*-propylazulene-1-carboxamide **[1]**, 3-methyl-*N*-butylazulene-1-carboxamide **[2]**, 3-methyl-*N*-pentylazulene-1-carboxamide **[3]**, 3-methyl-*N*-(2-hydroxyethyl)azulene-1-carboxamide **[4]**, 3-methyl-*N*-(3-hydroxypropyl) azulene-1-carboxamide **[5]**, 3-methyl-*N*-(2-methoxyethyl)azulene-1-carboxamide **[6]**, 3-methyl-*N*-(3-methoxypropyl)azulene-1-carboxamide **[7]**, 7-isopropyl-3-methyl-*N*-propylazulene-1-carboxamide **[8]**, 7-isopropyl-3-methyl-*N*-butylazulene-1-carboxamide **[9]**, 7-isopropyl-3-methyl-*N*-pentylazulene-1-carboxamide **[10]**, 7-isopropyl-3-methyl-*N*-(2-hydroxyethyl)azulene-1-carboxamide **[11]**, 7-isopropyl-3-methyl-*N*-(3-hydroxypropyl)azulene-1-carboxamide **[12]**, 7-isopropyl-3-methyl-*N*-(2-methoxyethyl)azulene-1-carboxamide **[13]**, 7-isopropyl-3-methyl-*N*-(3-methoxypropyl)azulene-1-carboxamide **[14]**, 2-methoxy-*N*-propylazulene-1-carboxamide **[15]**, 2-methoxy-*N*-butylazulene-1-carboxamide **[16]**, 2-methoxy-*N*-pentylazulene-1-carboxamide **[17]**, 2-methoxy-*N*-(2-hydroxyethyl)azulene-1-carboxamide **[18]**, 2-methoxy-*N*-(3-hydroxypropyl)azulene-1-carboxamide **[19]**, 2-methoxy-*N*-(2-methoxyethyl)azulene-1-carboxamide **[20]**, 2-methoxy-*N*-(3-methoxypropyl)azulene-1-carboxamide **[21]** (structures shown in Figure 1) were synthesized, according to previous reports (13-17). All compounds were dissolved in DMSO at 40 mM and stored at –20˚C before use.

Cell culture. Human normal oral cells (HGF, HPLF, HPC) cells (18) at 12~20 population doubling level (PDL) and OSCC cell lines (Ca9-22, HSC-2, HSC-3, HSC-4) (Riken Cell Bank, Tsukuba, Japan) were cultured at 37˚C in DMEM supplemented with 10% heat-inactivated FBS and antibiotics as described previously (11).

Assay for cytotoxic activity. Cells were inoculated at 2×10^3 cells/0.1 ml in a 96-microwell plate. After 48 h, the medium was replaced with 0.1 ml of fresh medium containing different concentrations of test compounds. Control cells were treated with the same amounts of DMSO present in each diluent solution. Cells were incubated for 48 h and the relative viable cell number was then determined by the MTT method, as described previously (11). The CC_{50} was determined from the dose–response curve of triplicate samples.

Calculation of tumor-specificity index (TS). TS was calculated as the ratio of mean CC_{50} (HGF+HPLF+HPC) to mean CC_{50} (Ca9-22+HSC-2+HSC-3+HSC-4), using seven cell lines [(D/B) in Table I] (19), and as the ratio of CC_{50} (HGF) to CC_{50} (Ca9-22) [(C/A) in Table I], using two cell lines derived from the gingival tissue (20). Normal keratinocytes, which are highly sensitive to many anticancer drugs (21), were not used in this study.

Table I. *Cytotoxicity of 21 azulene amide derivatives and doxorubicin against human oral squamous cell carcinoma cell lines and human oral normal cells.*

	CC_{50} (μM)												
	Human oral squamous cell carcinoma cell lines					Human normal oral cells				TS		PSE	
	(A) Ca9-22	HSC-2	HSC-3	HSC-4	(B) mean	(C) HGF	HPLF	HPC	(D) mean	(D/B)	(C/A)	$(D/B^2)\times100$	$(C/A^2)\times100$
Group A													
1	279	318	364	353	329	391	394	289	358	1.1	1.4	0.3	0.5
2	139	169	148	111	142	265	285	162	237	1.7	1.9	1.2	1.4
3	76	61	66	50	63	270	299	165	245	3.9	3.6	6.1	4.7
4	388	324	400	392	376	398	396	389	395	1.0	1.0	0.3	0.3
5	382	397	398	385	391	381	400	214	332	0.8	1.0	0.2	0.3
6	377	370	362	344	363	363	400	170	311	0.9	1.0	0.2	0.3
7	284	379	288	235	296	351	391	204	315	1.1	1.2	0.4	0.4
(mean)	275	288	289	267	280	346	366	227	313	1.5	1.6	1.2	1.1
Group B													
8	35	48	47	38	42	355	400	138	298	7.1	10.1	16.9	28.5
9	36	158	38	160	98	400	400	299	366	3.7	11.1	3.8	30.8
10	43	295	33	307	170	400	400	400	400	2.4	9.3	1.4	21.7
11	145	154	114	105	129	228	245	212	228	1.8	1.6	1.4	1.1
12	137	163	112	94	127	252	283	184	240	1.9	1.8	1.5	1.3
13	85	136	113	116	112	236	248	133	206	1.8	2.8	1.6	3.3
14	54	96	67	74	73	146	143	115	135	1.9	2.7	2.5	5.0
(mean)	76	150	75	128	107	288	303	212	268	2.9	5.6	4.2	13.1
DXR	10.10	1.40	3.29	0.08	3.72	344	349	209	301	80.9	34.1	2175.8	337.8
Group C													
15	176	144	109	82	128	285	285	319	296	2.3	1.6	1.8	0.9
16	124	114	77	69	96	258	196	246	233	2.4	2.1	2.5	1.7
17	53	75	81	61	67	155	183	137	158	2.3	2.9	3.5	5.6
18	400	400	376	387	391	400	400	400	400	1.0	1.0	0.3	0.3
19	376	400	380	393	387	400	400	400	400	1.0	1.1	0.3	0.3
20	323	400	358	365	361	400	339	400	380	1.1	1.2	0.3	0.4
21	235	387	283	274	295	354	349	366	356	1.2	1.5	0.4	0.6
(mean)	241	274	238	233	246	322	307	324	318	1.6	1.6	1.3	1.4
DXR	1.92	1.68	0.01	0.01	0.90	216.6	150.2	332.7	233.2	258.2	113.1	28586.9	5905.2

CC_{50} value was determined by dose-response experiments performed in triplicate. Ca9-22, HSC-2, HSC-3 and HSC-4: Oral squamous cell carcinoma cell lines; HGF: human gingival fibroblasts; HPLF: periodontal ligament fibroblasts; HPC: pulp cells; CC_{50}: 50% cytotoxic concentration, DXR: doxorubicin; TS: tumor-selectivity index; PSE: potency-selectivity expression.

Calculation of potency-selectivity expression (PSE). PSE was calculated by dividing TS value by CC_{50} against tumor cells (19) [$(D/B^2)\times100$ and $(C/A^2)\times100$] (Table I).

Western blot analysis. The cells were washed, lysed and their protein extracts subjected to western blot (WB) analysis, as described previously (11). The blots were probed with the primary antibody [antibodies against cleaved caspase-3 (Cell Signaling Technology Inc., Beverly, MD, USA), poly ADP-ribose polymerase (PARP) (Cell Signaling Technology Inc.) and glyceraldehyde 3-phosphate dehydrogenase (GAPDH, Trevigen, Gaithersburg, MD, USA), followed by incubation with a horseradish peroxidase-conjugated secondary antibody [α-rabbit IgG (DAKO, Tokyo Japan)]. The immune complexes were visualized using Pierce Western Blotting Substrate Plus (Thermo Fisher Scientific). WB results were documented and quantified using ImageQuant LAS 500 (GE Healthcare, Tokyo, Japan) (22).

Cell cycle analysis. Cells (approximately 10^6 cells) were harvested, fixed with paraformaldehyde (Wako) in PBS(-), treated with ribonuclease (RNase) A (Sigma-Aldrich Inc.), stained propidium iodide (PI) (Wako) in the presence of 0.01% NonidetP-40 (Nakalai Tesque Inc., Kyoto, Japan), filtered through Falcon® cell strainers (Corning, NY, USA) and then were subjected to cell sorting (SH800 Series, SONY Imaging Products and Solutions Inc., Atsugi, Kanagawa, Japan), as described previously (19). Cell cycle analysis was performed with Cell Sorter Software version 2.1.2. (SONY Imaging Products and Solution Inc.) (19).

Calculation of chemical descriptors. pCC_{50} (*i.e.*, the $-\log CC_{50}$) was used for the comparison of the cytotoxicity between the compounds, since the CC_{50} values had a distribution pattern close to a logarithmic normal distribution. The mean pCC_{50} values for normal cells and tumor cell lines were defined as **N** and **T**, respectively (23). The 3D-structure of each chemical structure was

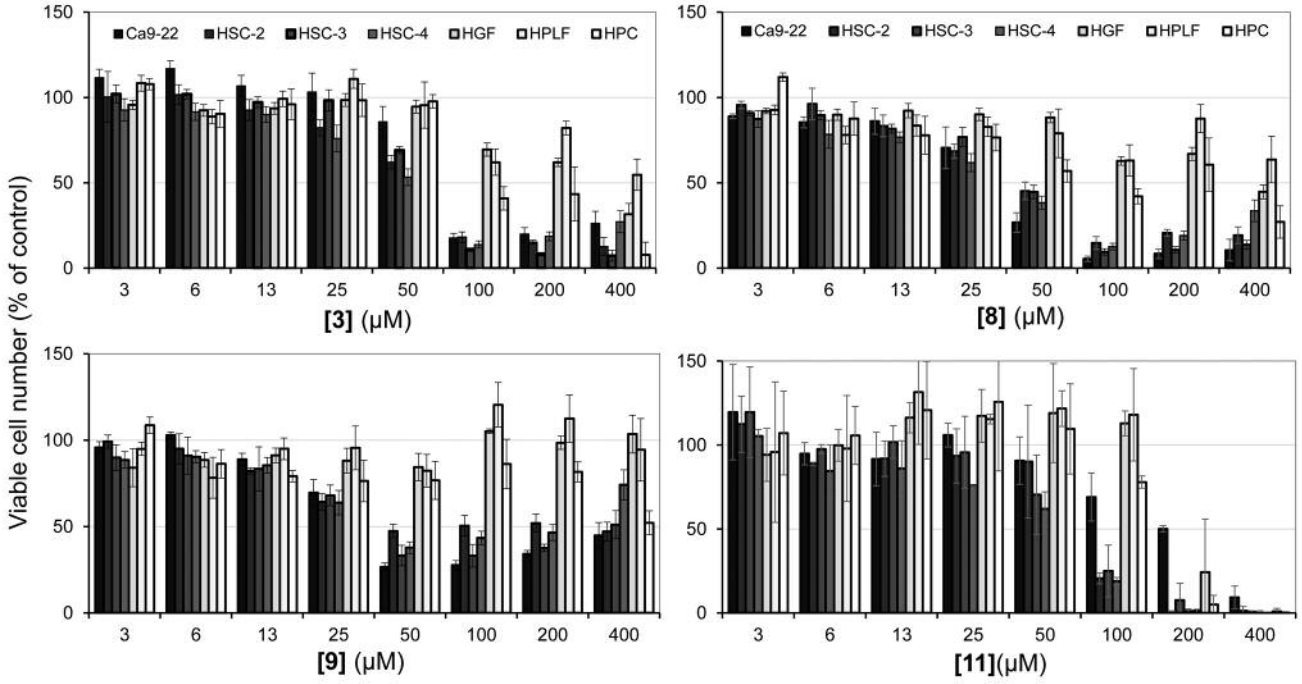

Figure 2. *Cytotoxicity of 3-methyl-N-pentylazulene-1-carboxamide **[3]**, 7-isopropyl-3-methyl-N-propylazulene-1-carboxamide **[8]**, 7-isopropyl-3-methyl-N-butylazulene-1-carboxamide **[9]** and 2-methoxy-N-pentylazulene-1-carboxamide **[17]** against human malignant and non-malignant cells. Human oral squamous cell carcinoma (OSCC) cell lines (Ca9-22, HSC-2, HSC-3, HSC-4) and human oral normal cells (HGF, HPLF, HPC) were treated for 48 h with the indicated concentrations of **[3]**, **[8]**, **[9]**, or **[17]** and viable cell number was determined by the MTT method. Each value represents mean±S.D. of triplicate assays.*

drawn by Marvin Sketch ver 16 (ChemAxon, Budapest, Hungary, http://www.chemaxon.com), and optimized by CORINA Classic (Molecular Networks GmbH, Nürnberg, Germany) with partial charge calculations (amber-10: EHT) in Molecular Operating Environment (MOE) version 2018.0101 (Chemical Computing Group Inc., Quebec, Canada) and Dragon (Dragon 7 version 7.0.2, Kode srl., Pisa, Italy).

Statistical analysis. Each experimental value was expressed as the mean±standard deviation (SD) of triplicate or quadruplicate measurements. The correlation between chemical descriptors and cytotoxicity or tumor specificity was investigated using simple regression analyses by JMP Pro version 14.0.0 (SAS Institute Inc., Cary, NC, USA). The significance level was set at $p<0.05$.

Results

Cytotoxicity. Twenty one azulene amides used in this study were classified into three groups, 3-methyl-*N*-alkylazulene-1-carboxamides **[1-7]** (Group A), 7-Isopropyl-3-methyl-*N*-alkylazulene-1-carboxamides **[8-14]** (Group B) and 2-methoxy-*N*-alkylazulene-1-carboxamides **[15-21]** (Group C) (Figure 1). We compared their cytotoxic activity against four human oral squamous cell carcinoma (OSCC) cell lines (Ca9-22, HSC-2, HSC-3, HSC-4) and three normal oral cells (HGF, HPLF, HPC), by comparing the 50% cytotoxic concentration (CC_{50}) determined from the dose-response curve (example shown in Figure 2) (Table I).

Generally, group B compounds showed higher cytotoxicity against OSCC cell lines (mean CC_{50}=107 μM) than group C (246 μM) and group A compounds (280 μM). Among 21 compounds, **[8]** showed the highest cytotoxicity (CC_{50}=42 μM), followed by **[3]** (63 μM) and **[17]** (67 μM). From the dose-response curve, **[3, 8, 17]** and **[9]** showed cytotoxic and cytostatic growth inhibition against four OSCC cell lines, respectively (Figure 2). On the other hand, group A, B and C compounds showed comparable cytotoxicity against normal oral cells (mean CC_{50}=313, 301 and 318 μM, respectively).

Tumor-specificity (TS). TS was determined by dividing the mean CC_{50} value towards the three normal cells by the mean CC_{50} value towards the four OSCC cell lines (D/B, Table I) or by dividing the CC_{50} value against HGF cells by the CC_{50} value against Ca9-22 cells, two cells derived from the gingival tissue (C/ A, Table I). Among Group A, **[3]** showed the highest tumor-specificity (TS=3.9 in D/B; 3.6 in C/A). Among Group B, **[8]** showed the highest tumor-specificity (TS= 7.1 in D/B; 10.1 in C/A), followed by **[9]** (TS=3.7, in D/B; 11.1 in C/A). Among Group C, **[17]** showed the highest tumor-specificity (TS=2.3 in D/B, 2.9 in C/A) (Table I).

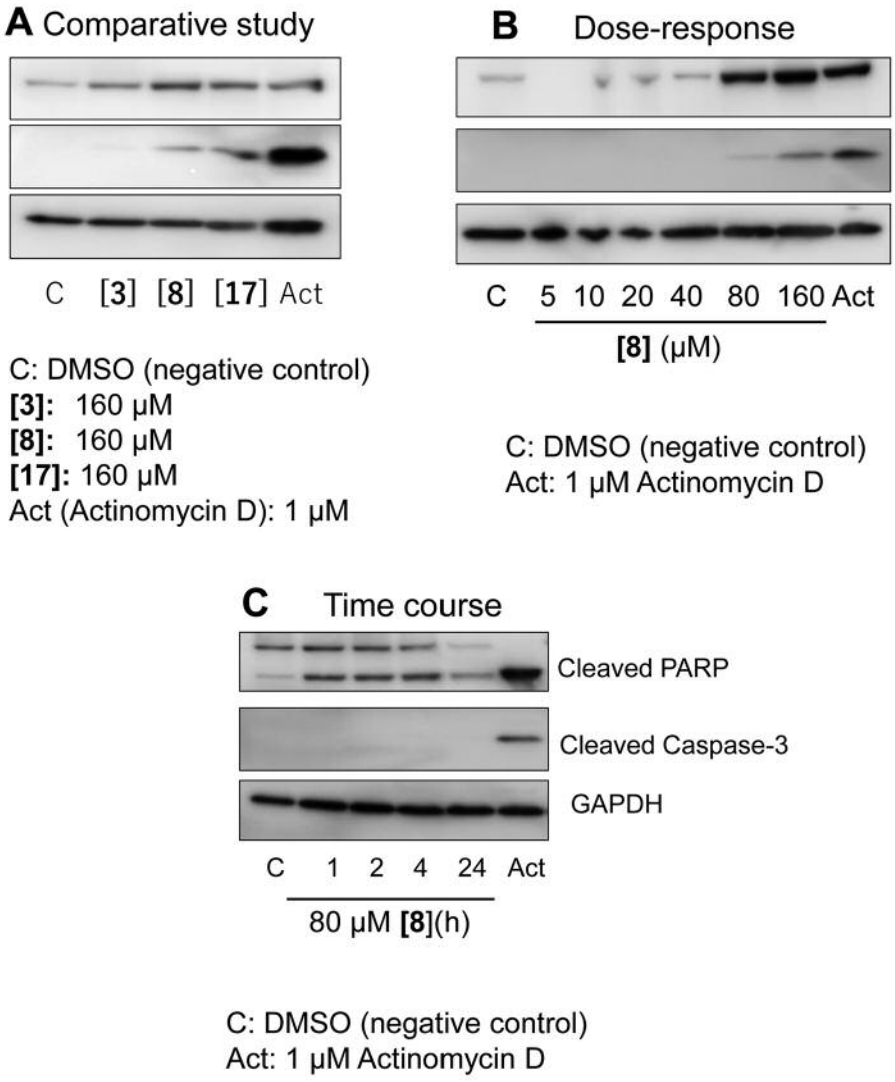

Figure 3. *Assessment of caspase-3 activation by **[3]**, **[8]**, or **[17]**. (A) Comparison between three compounds. (B) Dose-response and (C) time course of apoptosis induction by **[8]**. Ca9-22 cells were incubated for 24 h with the indicated concentrations of **[3]**, **[8]**, or **[17]** or 1 μM actinomycin D (Act D) as positive control and subjected to western blot analysis.*

PSE value. Next, the potency-selectivity expression (PSE) value that reflects both the cytotoxicity against OSCC and tumor-specificity was determined. **[8]** showed much higher PSE value [16.9 in (D/B^2) ×100; 28.5 in (C/A^2) ×100)], followed by **[3]** (PSE=6.1; 4.7), **[9]** (PSE=3.8; 30.8) and **[17]** (PSE=3.5; 5.6).

Apoptosis induction. Western blot analysis (Figure 3A) demonstrated that among **[3]**, **[8]**, and **[17]** compounds, **[8]** induced the cleavage of PARP, one of the substrates of caspase-3, most potently, followed by **[17]** and **[3]**, while **[17]** induced cleavage of caspase-3 (producing active form) most potently, followed by **[8]** and **[3]**. Dose-response study (Figure 3B) showed that cleavage of PARP by [8] was detected above 80 μM, while activation of capsase-3 was detected above 160 μM, suggesting the induction of apoptosis (24). Time course study (Figure 3C) shows that cleavage of PARP was observed at early stage (1, 2 and 4 h after treatment with 80 μM **[8]**), and declined thereafter (at 24 h).

Light microscopical observation (upper column, Figure 4) revealed that cells were damaged and began to detach by treatment with higher concentrations (160 or 200 μM) of all three compounds **[3, 8, 17]**. Both **[17]** and actinomycin D

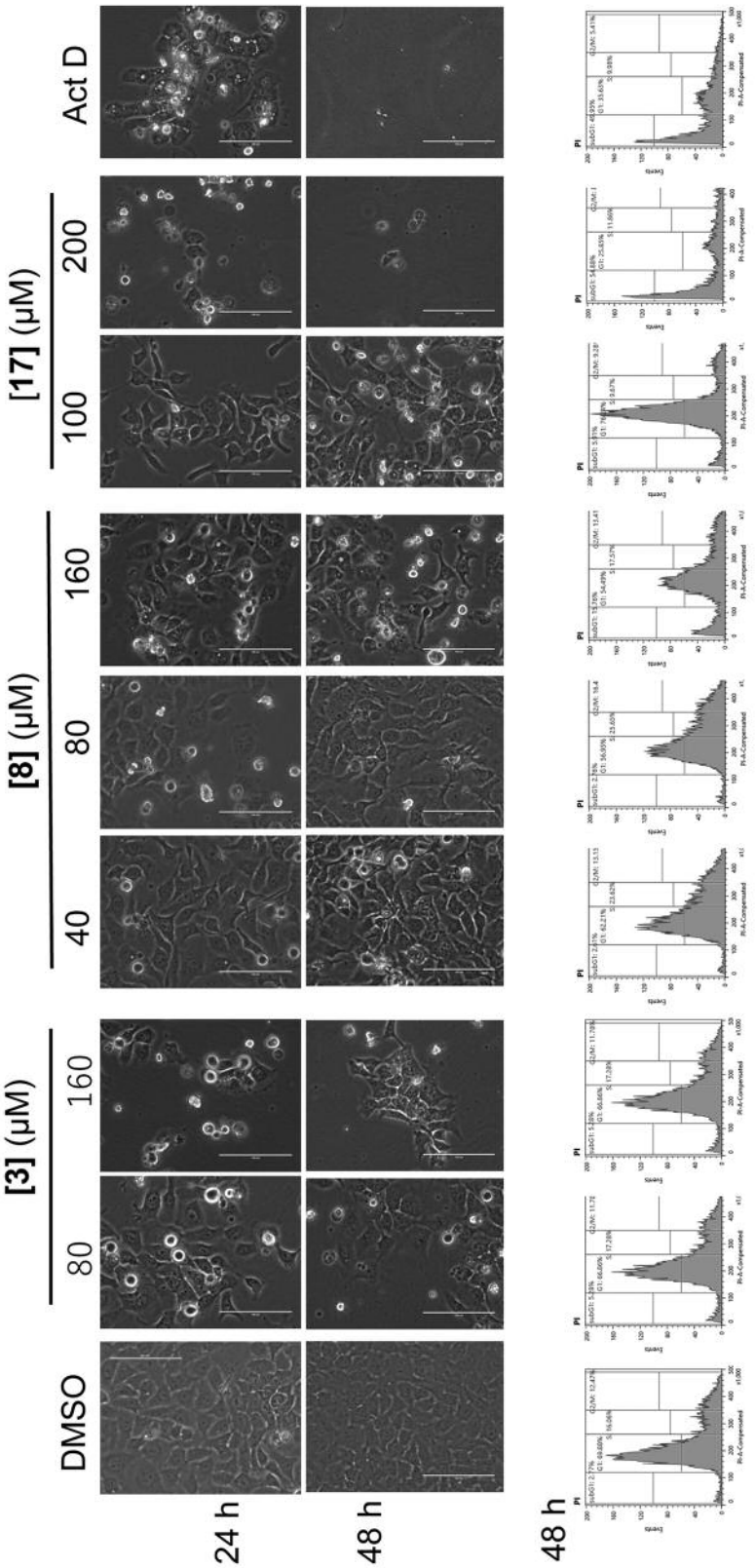

Figure 4. *Production of subG$_1$ population by **[3]**, **[8]**, or **[17]**. Ca9-22 cells were incubated for 24 or 48 h with the indicated concentrations of **[3]**, **[8]**, **[17]** or 1 μM actinomycin D (Act D) as a positive control and subjected to cell sorter analysis.*

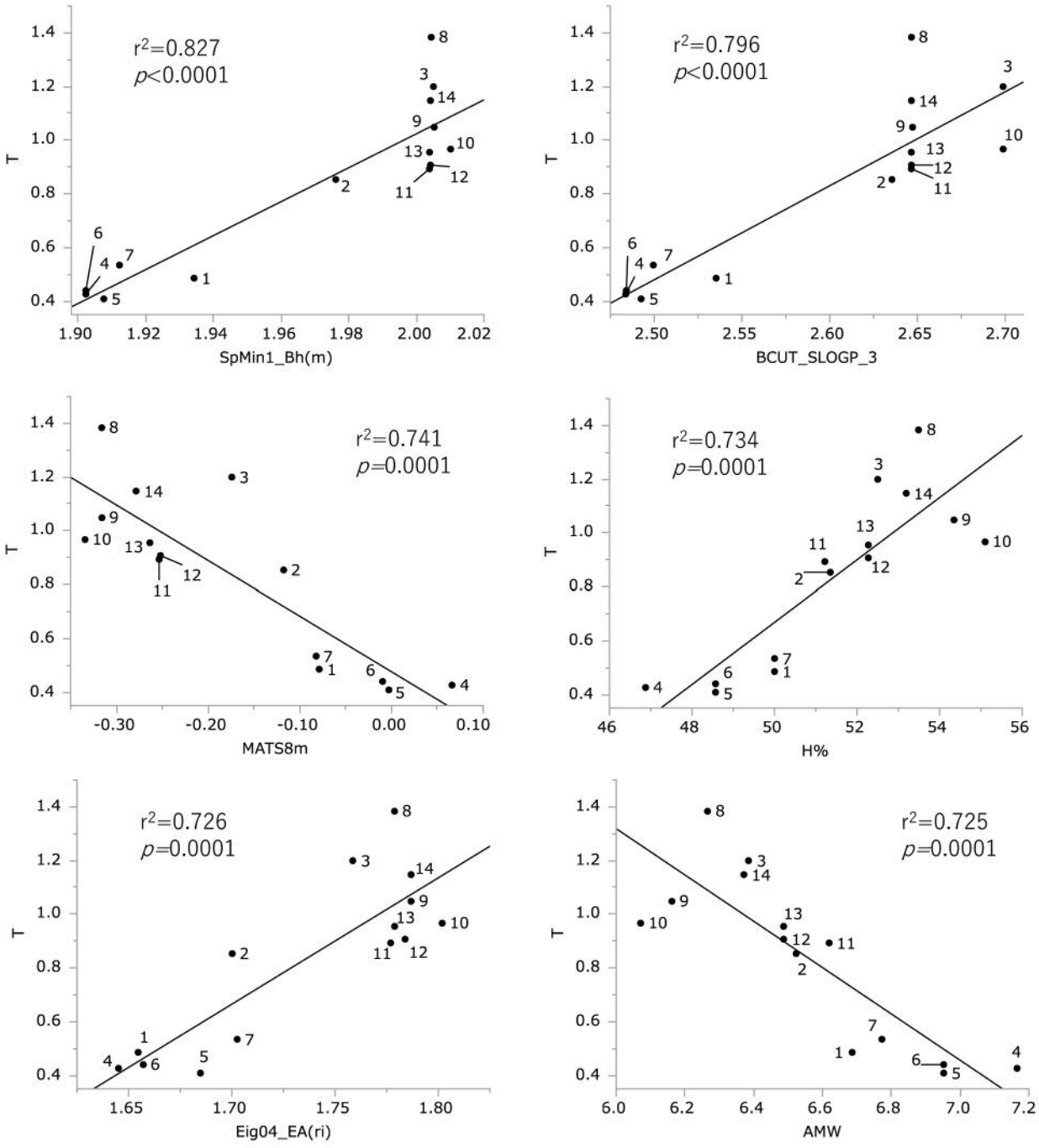

Figure 5. *Determination of coefficient between chemical descriptors and cytotoxicity of 14 Group A and B compounds against tumor cells (defined as T). The mean (pCC_{50} i.e., the $-\log CC_{50}$) values for tumor cell lines were defined as T.*

(positive control) produced apoptotic cells (upper column, Figure 4). Cell-cycle analysis demonstrated that **[17]** increased the subG1 cell population to an extent similar with that of actinomycin D, while **[8]** was slightly less potent in apoptosis induction (lower panel, Figure 4).

Computational analysis. Since 3-methyl-*N*-alkylazulene-1-carboxamides **[1-7]** (Group A), 7-Isopropyl-3-methyl-*N*-alkylazulene-1-carboxamides [**8-14**] (Group B) showed a higher tumor-specificity than 2-methoxy-*N*-alkylazulene-1-carboxamides **[15-21]** (Group C), QSAR analysis was

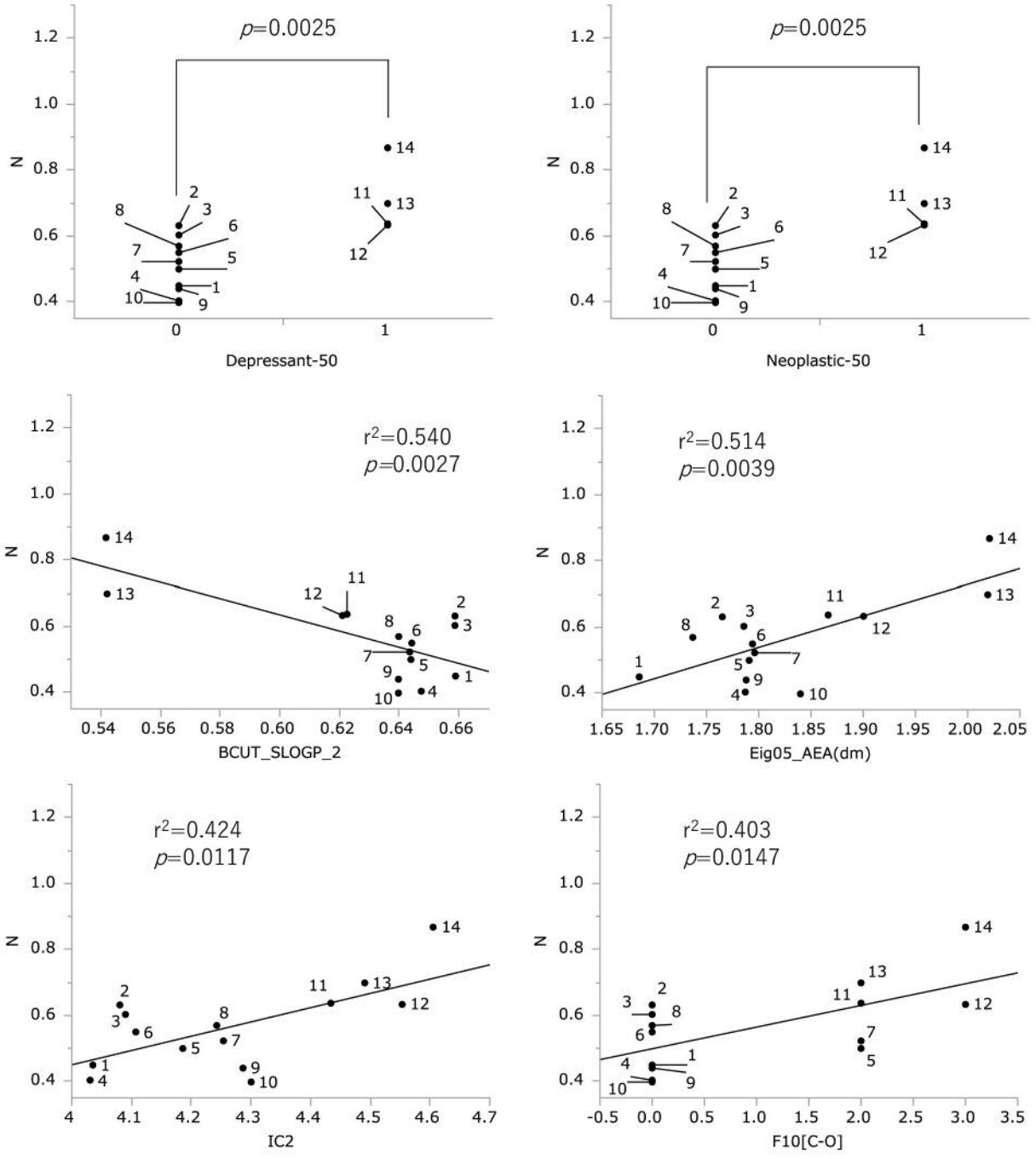

Figure 6. *Determination of coefficient between chemical descriptors and cytotoxicity of 14 Group A and B compounds against normal cells (defined as N). The mean (pCC_{50} i.e., the $-log\ CC_{50}$) values for normal cells were defined as N.*

performed with Group A and B compounds **[1-14]**. The number of descriptors calculated from MOE and dragon was 344 and 5,255, respectively. As a result of excluding duplicate descriptors, the number of descriptors reduced to 301 and 2,765, respectively. Among a total of 3,066 descriptors, the top six descriptors that showed the highest correlation coefficient (r^2) to **T**, **N** and **T-N** are shown in Table II.

Cytotoxicity against human OSCC cell lines was correlated with descriptors SpMin1_Bh(m) (topological shape) (r^2=0.827, p<0.0001), BCUT_SLOGP_3 (topological

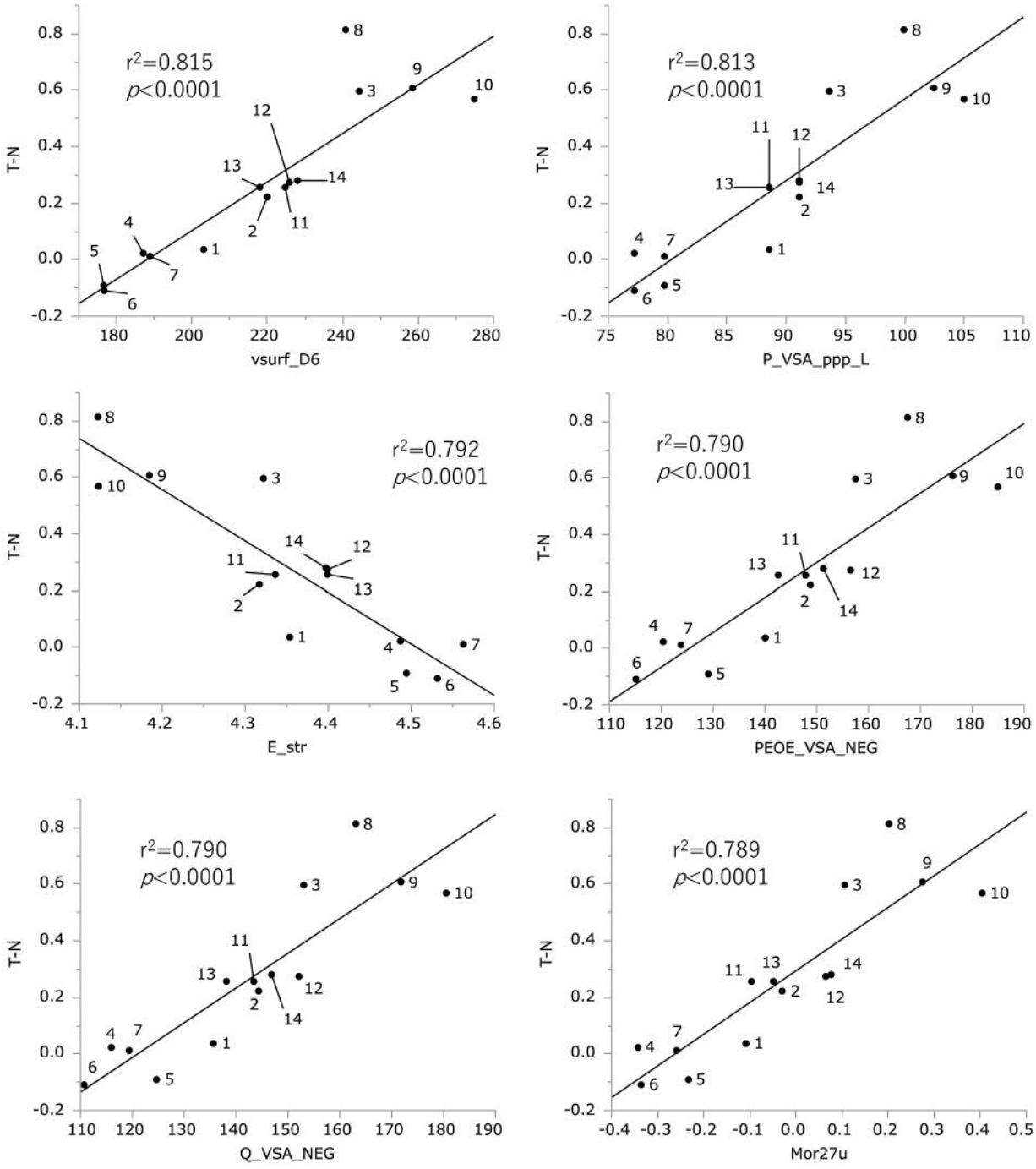

Figure 7. *Determination of coefficient between chemical descriptors and tumor specificity of 14 Group A and B compounds (defined as T−N).*

shape) (r^2=0.796, p<0.0001), MATS8m (topological shape and size) (r^2=0.741, p=0.0001), H% (percentage of H atoms) (r^2=0.734, p=0.0001), Eig04_EA(ri) (topological shape and energy) (r^2=0.726, p=0.0001), AMW (average molecular weight) (r^2=0.725, p=0.0001) (Figure 5).

Cytotoxicity against human normal oral mesenchymal cells was correlated with descriptors Depressant-50 (Drug-like indices) (p=0.0025), Neoplastic-50 (Drug-like indices) (p=0.0025), BCUT_SLOGP_2 (topological shape) (r^2=0.540, p=0.0027), Eig05_AEA(dm) (topological shape

Table II. *Top six chemical descriptors that correlate with cytotoxicity to tumor cells, normal cells and tumor-specificity (having the highest r^2 values).*

	Descriptor	Source	Meaning	Category	Explanation
T	SpMin1_Bh(m)	Dragon	Topological shape	Burden eigenvalues	Smallest eigenvalue n. 1 of Burden matrix weighted by mass
	BCUT_SLOGP_3	MOE	Topological shape	Adjacency and distance matrix descriptors	The BCUT descriptors using atomic contribution to logP (using the Wildman and Crippen SlogP method) instead of partial charge.
	MATS8m	Dragon	Topological shape and size	2D autocorrelations	Moran autocorrelation of lag 8 weighted by mass
	H%	Dragon	Percentage of H atoms	Constitutional indices	Percentage of H atoms
	Eig04_EA(ri)	Dragon	Topological shape and energy	Edge adjacency indices	Eigenvalue n. 4 from edge adjacency mat. weighted by resonance integral
	AMW	Dragon	Average molecular weight	Constitutional indices	Average molecular weight
N	Depressant-50	Dragon	Drug-like indices	Drug-like indices	Ghose-Viswanadhan-Wendoloski antidepressant-like index at 50%
	Neoplastic-50	Dragon	Drug-like indices	Drug-like indices	Ghose-Viswanadhan-Wendoloski antineoplastic-like index at 50%
	BCUT_SLOGP_2	MOE	Topological shape	Adjacency and distance matrix descriptors	The BCUT descriptors using atomic contribution to logP (using the Wildman and Crippen SlogP method) instead of partial charge.
	Eig05_AEA(dm)	Dragon	Topological shape and dipole moment	Edge adjacency indices	Eigenvalue n. 5 from augmented edge adjacency mat. weighted by dipole moment
	IC2	Dragon	Topological shape	Information indices	Information Content index (neighborhood symmetry of 2-order)
	F10[C-O]	Dragon	Topological shape	2D atom pairs	Frequency of C - O at topological distance 10
T-N	vsurf_D6	MOE	3D shape and size	Surface area, volume and shape descriptors	Hydrophobic volume (8 descriptors)
	P_VSA_ppp_L	Dragon	Topological shape and lipophilicity	P_VSA-like descriptor	P_VSA-like on potential pharmacophore points, L - lipophilic
	E_str	MOE	3D shape and energy	Potential Energy descriptors	Bond stretch potential energy. In the Potential Setup panel, the term enable (Bonded) flag is ignored, but the term weight is applied.
	PEOE_VSA_NEG	MOE	Topological shape and partial charge	Partial charge descriptors	Total negative van der Waals surface area. This is the sum of the vi such that qi is negative. The vi are calculated using a connection table approximation.
	Q_VSA_NEG	MOE	Topological shape and partial charge	Partial charge descriptors	Total negative van der Waals surface area. This is the sum of the vi such that qi is negative. The vi are calculated using a connection table approximation.
	Mor27u	Dragon	3D shape and size	3D-MoRSE descriptors	Signal 27/unweighted

and dipole moment) (r^2=0.514, p=0.0039), IC2 (topological shape) (r^2=0.424, p=0.0117), F10[C-O] (topological shape) (r^2=0.403, p=0.0147) (Figure 6).

Tumor specificity was correlated with descriptors vsurf_D6 (3D shape and size) (r^2=0.815, p<0.0001), P_VSA_ppp_L (topological shape and lipophilicity) (r^2=0.813, p<0.0001), E_str (3D shape and energy) (r^2=0.792, p<0.0001), PEOE_VSA_NEG (topological shape and partial charge) (r^2=0.790, p<0.0001), Q_VSA_NEG (topological shape and partial charge) (r^2=0.790, p<0.0001), Mor27u (3D shape and size) (r^2=0.789, p<0.0001) (Figure 7).

Discussion

The present study demonstrated that 7-isopropyl-3-methyl-*N*-alkylazulene-1-carboxamides **[8-14]** (Group B) showed slightly higher OSCC-specific cytotoxicity than 3-methyl-*N*-alkylazulene-1-carboxamides **[1-7]** (Group A) and 2-methoxy-*N*-alkylazulene-1-carboxamides **[15-21]** (Group C). Among them, 7-isopropyl-3-methyl-*N*-propylazulene-1-carboxamide **[8]** showed the highest tumor-specificity towards OSCC over normal oral cells, based on TS and PSE values. **[8]** induced apoptosis markers such as caspase-3

activation (24) and production of subG1 population (25) only at 160 μM (Figure 3), four times the CC_{50} (42 μM) (Table I). On the other hand, **[17]**, that showed lower tumor-specificity than **[8]** (TS=2.3 *vs*. 7.1 (D/B), 2.9 *vs*. 10.1 (C/A); PSE=3.5 *vs*. 16.9 in $(D/B^2)\times100$, 5.6 *vs*. 28.5 in $C/A^2)\times100$) (Table I), activated caspase-3 and produced a higher subG1 population (Figure 4). These data suggest that induction of tumor-specific cytotoxicity (anti-tumor activity) by **[8]** may not be mediated *via* apoptosis induction. There are many types of cell death, such as intrinsic and extrinsic apoptosis, oncosis, necroptosis, parthanatos, ferroptosis, sarmoptosis, autophagic cell death, autosis, autolysis, paraptosis, pyroptosis, phagoptosis, and mitochondrial permeability transition (26). Further study is required to investigate the possibility of the involvement of necrotic cell death, such as pyroptosis and necroptosis, in which the activation of caspase-1, IL-1β and IL-18IL-pathways is involved (27).

QSAR analysis with 14 Group A and B compounds demonstrated that their tumor-specificity was correlated with molecular shape (descripted by vsurf_D6, P_VSA_ppp_L, E_str, PEOE_VSA_NEG, Q_VSA_NEG, Mor27u) and lipophilicity (descripted by P_VSA_ppp_L) (Table II). We also reported previously that tumor-specificity of ten *N*-alkylguaiazulenecarboxamides was correlated with molecular shape (descripted by vsurf_ID1, vsurf_ID5, vsurf_ID4, vsurf_CW4, vsurf_ID3, vsurf_CW3) and hydrophobicity (descripted by vsurf_ID1, vsurf_ID5, vsurf_ID4, vsurf_ID3) (11). These data suggest that the antitumor-potential of guaiazulenes can be estimated by their molecular shape and hydrophobicity. By closer inspection, [**9**] (100~400 μM) and **[17]** (13~100 μM) were found to stimulate the growth of normal oral cells. The biological significance of this hormetic growth stimulation (28) remains to be investigated.

[8] and **[9]** have similar chemical structure to guaiazulene (1,4-dimethyl-7-isopropylazulene), all of them having isopropyl group in seven-membered ring and methyl group at the different positions. As far as we know only two studies have been published on the anticancer activity against OSCC (8, 29). More tumor-specific derivatives of **[8]** as a lead compound are being synthesized to examine their anti-cancer effects.

Conflicts of Interest

The Authors confirm that there are no known conflicts of interest associated with this publication and there was no significant financial support for this work that could have influenced its outcome.

Author's Contributions

Hiroshi Sakagami designed the study and wrote the draft of the manuscript Masashi Hashimoto and Hidetsugu Wakabayashi synthesized all compounds. Hidetsugu Wakabayashi supervised the overall study and revised the manuscript. Kana Imanari and Noriyuki Okudaira performed the western blot analysis. Kenjiro Bandow, Mineko Tomomura and Akito Tomomura performed the cell cycle analysis. Junko Nagai and Yoshihiro Uesawa performed the QSAR analysis.

Acknowledgements

This work was partially supported by KAKENHI from the Japan Society for the Promotion of Science (JSPS) (16K11519).

References

1 Kalil DM, Silvestro LS and Austin PN: Novel preoperative pharmacologic methods of preventing postoperative sore throat due to tracheal intubation. AANA J *82(3)*: 188-197, 2014. PMID: 25109156.

2 Sakai H and Misawa M: Effect of sodium azulene sulfonate on capsaicin-induced pharyngitis in rats. Basic Clin Pharmacol Toxicol *96(1)*: 54-59, 2005. PMID: 15667596. DOI: 10.1111/j.1742-7843.2005.pto960108.x

3 Ge ZD, Auchampach JA, Piper GM and Gross GJ: Comparison of cardioprotective efficacy of two thromboxane A2 receptor antagonists. J Cardiovasc Pharmacol *41(3)*: 481-488, 2003. PMID: 12605028.

4 Asato AE, Peng A, Hossain MZ, Mirzadegan T and Bertram JS: Azulenic retinoids: novel nonbenzenoid aromatic retinoids with anticancer activity. J Med Chem *36(21)*: 3137-3147, 1993. PMID: 8230100.

5 Kourounakis AP, Rekka EA and Kourounakis PN: Antioxidant activity of guaiazulene and protection against paracetamol hepatotoxicity in rats. J Pharm Pharmacol *49(9)*: 938-942, 1997. PMID: 9306266.

6 Kourounakis AP, Rekka EA and Kourounakis PN: Effect of guaiazulene on some cytochrome P450 activities. Implication in the metabolic activation and hepatotoxicity of paracetamol. Arch Pharm (Weinheim) *330(1-2)*: 7-11, 1997. PMID: 9112807.

7 Li P, Liu X, Zhu H, Tang X, Shi X, Liu Y and Li G: Unusual inner-salt guaiazulene alkaloids and bis-sesquiterpene from the South China Sea Gorgonian *Muriceides collaris*. Sci Rep *7(1)*: 7697, 2017. PMID: 28794492. DOI: 10.1038/s41598-017-08100-z

8 Wakabayashi H, Hashiba K, Yokoyama K, Hashimoto K, Kikuchi H, Nishikawa H, Kurihara T, Satoh K, Shioda S, Saito S, Kusano S, Nakashima H, Motohashi N and Sakagami H: Cytotoxic activity of azulenes against human oral tumor cell lines. Anticancer Res *23(6C)*: 4747-4755, 2003. PMID: 14981922.

9 Togar B, Turkez H, Hacimuftuoglu A, Tatar A and Geyikoglu F: Guaiazulene biochemical activity and cytotoxic and genotoxic effects on rat neuron and N2a neuroblastom cells. J Intercult Ethnopharmacol *4(1)*: 29-33, 2015. PMID: 26401381. DOI: 10.5455/jice.20141124062203

10 Fiori J, Teti G, Gotti R, Mazzotti G and Falconi M: Cytotoxic activity of guaiazulene on gingival fibroblasts and the influence of light exposure on guaiazulene-induced cell death. Toxicol In Vitro *25(1)*: 64-72, 2011. PMID: 20854889. DOI: 10.1016/j.tiv.2010.09.008

11 Wada T, Maruyama R, Irie Y, Hashimoto M, Wakabayashi H, Okudaira N, Uesawa Y, Kagaya H and Sakagami H: *In vitro* anti-tumor activity of azulene amide derivatives. In Vivo *32(3)*: 479-486, 2018. PMID: 29695549.

12 Hannun YA: Apoptosis and the dilemma of cancer chemotherapy. Blood *89(6)*: 1845-1853, 1997. PMID: 9058703.
13 Yasunami M, Miyoshi S, Kanegae N and Takase K: A versatile synthetic method of 1-alkylazulenes and azulene by the reaction of 3-methoxycarbonyl-2*H*-cyclohepta[**b**]furan-2-one with in site generated enamines. Bull Chem Soc Jpn *66*: 892-899, 1993.
14 Mathias LJ and Overberger CG: Simple syntheses of 1,3-bis(perfluoroacyl)azulenes and 1,3-azulenedicarboxylic acid. J Org Chem *45*: 1701-1703, 1980.
15 Doukas PH and Speaker TJ: Azulene analogs of pharmacologic agents I: amides. J Pharm Sci *60*: 184-189, 1971. PMID: 5572437.
16 Anderson AG and Anderson RG: The reaction of azulenes with trifluoro- and trichloroacetic anhydride. J Org Chem *27*: 3578-3581, 1962.
17 Nozoe T, Wakabayashi H, Shindo K, Ishikawa S, Wu CH and Yang PW: A convenient, one-pot azulene synthesis from cyclohepta[**b**]furan-2-ones and vinyl ether and its analogues (III) orthoesters as reagent. Heterocycles *32*: 213-220,1991.
18 Kantoh K, Ono M, Nakamura Y, Nakamura Y, Hashimoto K, Sakagami H and Wakabayashi H: Hormetic and anti-radiation effects of tropolone-related compounds. In Vivo *24(6)*: 843-851, 2010. PMID: 21164042.
19 Shi H, Nagai J, Sakatsume T, Bandow K, Okudaira N, Sakagami H, Tomomura M, Tomomura A, Uesawa Y, Takao K and Sugita Y: Quantitative structure–cytotoxicity relationship of 2-(*N*-cyclicamino) chromone derivatives. Anticancer Res *38(7)*: 3897-3906, 2018. PMID: 29970510. DOI: 10.21873/anticanres.12674
20 Horikoshi M, Kimura Y, Nagura H, Ono T and Ito H: A new human cell line derived from human carcinoma of the gingiva. I. Its establishment and morphological studies. Jpn J Oral Maxillofac Surg *20*: 100-106, 1974.
21 Sakagami H, Okudaira N, Masuda Y, Amano O, Yokose S, Kanda Y, Suguro M, Natori T, Oizumi H and Oizumi T: Induction of apoptosis in human oral keratinocyte by doxorubicin. Anticancer Res *37(3)*: 1023-1029, 2017. PMID: 28314260. DOI: 10.21873/anticanres.11412
22 Tomikoshi Y, Nomura M, Okudaira N, Sakagami H and Wakabayashi H: Enhancement of cytotoxicity of three apoptosis-inducing agents against human oral squamous cell carcinoma cell line by benzoxazinotropone. In Vivo *30(5)*: 645-650, 2016. PMID: 27566085.
23 Nagai J, Shi H, Kubota Y, Bandow K, Okudaira N, Uesawa Y, Sakagami H, Tomomura M, Tomomura A, Takao K and Sugita Y: Quantitative structure–cytotoxicity relationship of pyrano[4,3-b]chromones. Anticancer Res *38*: 4449-4457, 2018. PMID: 30061209. DOI: 10.21873/anticanres.12747
24 Bressenot A, Marchal S, Bezdetnaya L, Garrier J, Guillemin F and Plénat F: Assessment of apoptosis by immunohistochemistry to active caspase-3, active caspase-7, or cleaved PARP in monolayer cells and spheroid and subcutaneous xenografts of human carcinoma. J Histochem Cytochem *57(4)*: 289-300, 2009. PMID: 19029405. DOI: 10.1369/jhc.2008.952044
25 Kim IH, Kwon MJ and Nam TJ: Differences in cell death and cell cycle following fucoidan treatment in high-density HT-29 colon cancer cells. Mol Med Rep *15(6)*: 4116-4122, 2017. PMID: 28487956. DOI: 10.3892/mmr.2017.6520
26 Fricker M, Tolkovsky AM, Borutaite V, Coleman M and Brown GC: Neuronal Cell Death. Physiol Rev *98(2)*: 813-880, 2018. PMID: 29488822. DOI: 10.1152/physrev.00011.2017
27 Frank D and Vince JE: Pyroptosis *versus* necroptosis: similarities, differences, and crosstalk. Cell Death Differ *26(1)*: 99-114, 2019. PMID: 30341423. DOI: 10.1038/s41418-018-0212-6
28 Calabrese EJ: Biphasic dose responses in biology, toxicology and medicine: accounting for their generalizability and quantitative features. Environ Pollut *182*: 452-460, 2013. PMID: 23992683. DOI: 10.1016/j.envpol.2013.07.046
29 Uehara M, Minemura H, Ohno T, Hashimoto M, Wakabayashi H, Okudaira N and Sakagami H: *In vitro* antitumor activity of alkylaminoguaiazulenes. In Vivo *32(3)*: 541-547, 2018. PMID: 29695558.

Received March 18, 2019
Revised April 12, 2019
Accepted April 15, 2019